MICROPROBE MONAZITE DATING AND THE AGES OF SOME GRANITIC AND METAMORPHIC ROCKS FROM SOUTHEASTERN BRAZIL

SILVIO ROBERTO FARIAS VLACH AND GUILHERME AUGUSTO ROSA GUALDA

ABSTRACT Electron microprobe monazite crystallization ages are presented for selected granite and metamorphic rock samples from the Socorro and Guaxupé Nappes and the Alto Rio Grande and Ribeira Belts, southeastern Brazil. Results are consistent with ages close to 625 Ma of the main metamorphic episode in the nappe structures. Anatetic granite magmatic events in these terranes and in the Alto Rio Grande Belt were roughly coeval, most samples sharing ages between 610-625 (± 15) Ma. A crust-derived granite and a granite contact aureole from the Ribeira Belt have ages of 600-608 (± 15) Ma., suggesting that the main granite magmatism in this belt was somewhat younger, probably contemporaneous with the late orogenic phase in the nappe domains. Some regional and granite samples from all these terranes point to possible inheritance or incompletely homogenized monazite grains and intra-grain domains giving older ages, up to 690 *Ma.* The microprobe age results agree very well with independent isotopic data, reinforcing the applicability of the method to highlight an overall picture of main geochronological trends within the continental crust. The high spatial resolution of the probe should play an important role in understanding geochronological patterns of metasedimentary rocks and related migmatites and granites, as these rocks and their minerals often present chemical and isotopic domains related to contrasting geological events, not always recognized by conventional dating schemes.

Keywords: Electron probe microanalyser dating, monazite, metapelites, anatectic granites

INTRODUCTION

Chemical dating of Th/U rich minerals by electron probe microanalysis (EPMA) has been proved in the last few years to be a powerful and fast technique (Susuki and Adachi 1991, Montel *et al.* 1996, Rhede *et al.* 1996, Vlach *et al.* 1999). The high spatial resolution of the EPMA beam gives information about complex mineral zoning and overgrowths down to a few mm^3 and users are also able to see exactly what they are analyzing. These are very important features, as different textural generations of a Th-U mineral in a rock, or even domains within a single grain, can preserve chemical and isotopic signatures related to contrasting geological events. The method is non-destructive, sample preparation and analytical procedures are relatively easy and inexpensive and dating can be undertaken in a normal EPMA work procedure. On the other hand, not all rocks contain minerals suitable for dating and the age precision is, in most cases, about one order of magnitude poorer than the equivalent obtained by conventional U-Pb and other isotopic methods.

Monazite is very appropriated for EPMA dating. Th and U concentrations are high enough to produce measurable radiogenic Pb contents in most crystals older than 70-100 Ma. The closure temperature is up to 700-750° C (Parrish 1990), and metamictization effects are weak, even for relatively old and Th (U)-rich monazite, owing to the stability of Pb within its structure (Podor and Cuney 1997). In addition, it is a common accessory phase in peraluminous granites and medium- to high-grade metamorphic rocks, also appearing as a residual mineral in (meta)psammites.

We present a summary of procedures for monazite EPMA analysis and dating, as well as applications and interpretation potentials by considering the example of some Neoproterozoic granites, and regional and aureole metamorphic rocks from São Paulo State and nearby regions, in southeastern Brazil.

SAMPLING AND METHODOS

Neoproterozoic granitic and metamorphic rocks of the Socorro and Guaxupé (Varginha) Nappe terranes and of the Alto Rio Grande and Ribeira Belts, covering a wide area to the south of the São Francisco Craton, southeastern Brazil, were selected for this work (Fig. 1; see also Campos Neto and Caby 1999, Janasi 1999, and references therein). Samples come from the Pinhal (PH), Morungaba (Areia Branca Pluton, MO), Nazaré Paulista (NP), and Piedade (PD) crustal granites, gneisses and granulites, and the contact aureole rocks around the rapakivi-like Sorocaba Granite (SO).

Granites from the nappe structures are slightly peraluminous, equigranular, medium-grained biotite (PH,MO) and biotite-bearing garnet (NP) monzogranites. PD is a coarse-grained peraluminous biotite-rich porphyritic monzogranite with K-feldspar megacrystals. Sampled metamorphic rocks comprise medium- to high-grade cordierite (-sillimanite)-bearing biotite-garnet gneisses from the Socorro Nappe and a coarse-grained rutile-bearing kyanite-garnet granulite from the Guaxupé (Varginha) Nappe. SO is a fine-grained garnet-cordierite-biotite hornfels re-crystallized from low-grade metapelites of the São Roque Group.

Monazite appears in thin sections mostly as small (0.1-0.3 mm wide), typically rounded and clean grains included within biotite and garnet and to a lesser extent in feldspars, cordierite, and other accessories; large isolated grains are rare and restricted to some of the granite samples. Idiomorphic crystals were found only in Morungaba granites. The PD monazite is anhedral, has complex zoning, and often shows clean rims around a somewhat clouded core. Rock textures suggest that monazite is a relatively early crystallizing phase in all these granites.

Chemical age models

The Pb content in a Th-U-Pb closed system after an elapsed time *t* is given by the equation:

$$Pb_{meas} = Pb_0 + Th_{meas} \times \frac{A_b(^{232}Th) \times A_r(^{208}Pb)}{A_r(Th)} \times \left(\exp\left(^{232}\lambda_{Th} t\right) - 1\right) +$$
$$+ U_{meas} \times \left[\frac{A_b(^{238}U) \times A_r(^{206}Pb)}{A_r(U)} \times \left(\exp\left(^{238}\lambda_U t\right) - 1\right) + \frac{A_b(^{235}U) \times A_r(^{207}Pb)}{A_r(U)} \times \left(\exp\left(^{235}\lambda_U t\right) - 1\right) \right] \quad (1)$$

which can be also written in the form $a.Th_{meas} + b.U_{meas} - Pb_{meas} + Pb_0 = 0$. Elemental concentration (means) and Pb_0 are given in wt. %; A_b, A_r, and λ, stand for atomic abundance, atomic weights and decay constants (yr^{-1}), respectively; Pb_0 is the initial (common) Pb, and *t* is given in years. This equation can be solved for *t* in three ways as briefly described below.

A direct *t* solution for each Th-U-Pb measured triad is possible when Pb_0 is known or negligible in relation to total Pb. The date for a given sample is then computed by averaging all individual results within a statistically significant population (*e.g.*, Montel *et al.* 1996). On the other hand, if Pb_0 is constant within a data set, (1) is the equation of a plane in Th-U-Pb space. Significant fitting results for *a* and *b* coefficients and Pb_0 can be computed when there is a good dispersion of Th-U-Pb contents, given rise to independent *t* solutions for both the Th-Pb and U-Pb decay series (Rhede *et al.* 1996). The Th-Pb age can be computed by the well-known equation:

$$t_{(Th-Pb)} = \frac{1}{^{232}\lambda_{Th}} \times \ln\left[1 + a \times \frac{A_r\left(^{232}Th\right)}{A_r\left(^{208}Pb\right)}\right] \quad (2)$$

and an equivalent equation involving the *b* coefficient is used for the $t_{(U-Pb)}$ calculation.

The above method fails for minerals with high Th/U or U/Th ratios showing significant variations in Th or U contents, but not both. An alternative is the CHIME approach developed by Suzuki and Adachi (1991). Equalizing the second and third right-hand terms in (1) for a given *t*, measured U values can be converted into *equivalent* Th contents to obtain a Th* parameter, which is Th_{meas} plus the Th equivalent to U_{meas}, or a U* quantity can be calculated, by transforming Th into equivalent U contents. In this way, either the *a* or the *b* coefficient will disappear, turning (1) linear in Th*-Pb or U*-Pb coordinates. An iterative procedure combining equations (1) and (2), conveniently modified for Th* (U*), permits to find the best Th* (U*) and *t* values for an isochronic data set of a given sample.

Isochronic planar or linear results do not depend on Pb_0, *provided* it is constant, an assumption that is not always valid. It can also be shown that the age results are not affected by minor systematic errors,

Instituto de Geociências, Universidade de São Paulo, C.P. 11.348, 05422-970, São Paulo, Brazil. E-mail: srfvlach@usp.br

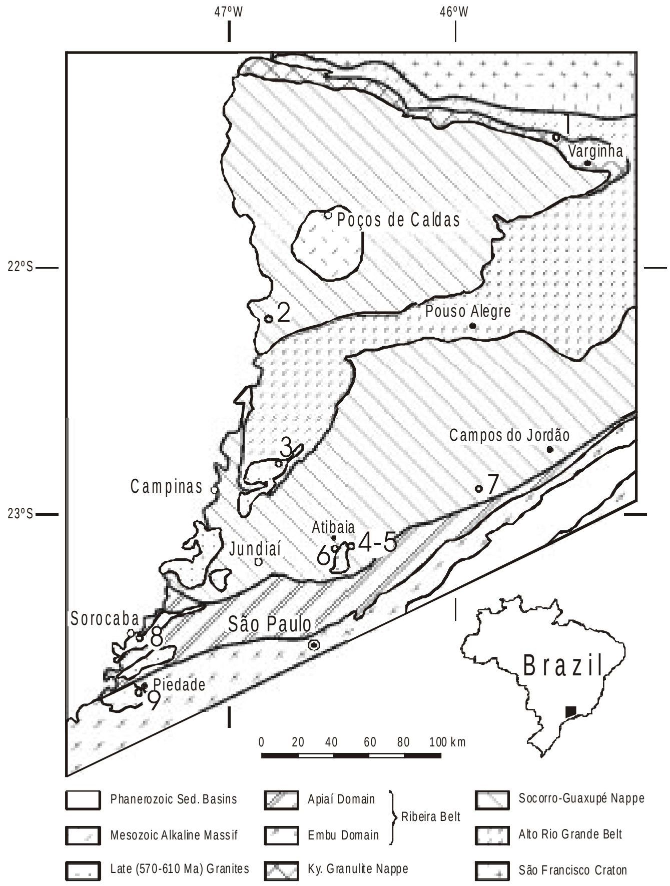

Figure 1 - Geological sketch map showing the main geologic units to the south of the São Francisco Craton, SE Brazil. Studied samples are as follows: 1: Varginha granulite; 2: Pinhal granite; 3: Areia Branca granite (Morungaba); 4 and 5: Atibaia gneisses; 6: Nazaré Paulista granite; 7: São Francisco Xavier gneiss; 8: Sorocaba contact aureole; 9: Piedade granite.

adding or subtracting constant values to the amounts of Th, Pb, or U. On the other hand, direct solutions are reliable only if the Pb_0 contents can be constrained. Theoretical considerations show that Pb can be incorporated within monazite Ca sites at the time of crystallization (Podor and Cuney 1997). However, most available data show that Pb_0 is very low compared to total Pb in monazite from most common rock types (up to a few ppm, *cf*. Parrish 1990, Crowley and Ghent 1999). Taking into account Pb probe measurement errors (about 80-100 ppm, see below), an initial work premise of a negligible or roughly constant Pb_0 content seems to be perfectly acceptable. Whatever the approach, results should be considered *a priori* as *dates*, with geological meaning, and so the *status* of *ages*, only if the considered isotopic system remained closed and Pb_0 constraints are valid.

Application examples of these models are presented and discussed in the next section. We developed a spreadsheet procedure to compute pertinent Th*, U*, individual dates and related uncertainties from elemental measurements and respective errors. Planar and linear chemical isochrons were fitted with the IsoPlot software (K.R. Ludwig). Other results are presented by means of age distribution diagrams, displaying the Gaussian probability density function of each measurement, the sum of all these individuals, a kind of "weighted histogram", and the probability function for the statistical averaged populations in a sample (see details in Montel *et al.* 1996).

Analytical procedures The analysis was carried on polished thin sections, with a 25 nm thick carbon coating, using a JEOL-8600 probe and a NORAN/Voyager EDS and WDS automation system. Instrumental conditions were set at 15 kV, 300 nA, and 2-5 mm for the accelerating voltage, beam current, and diameter, respectively, in order to improve the spatial resolution, X-ray signals and absorption corrections. Most of the tested clean monazite grains remained stable up to 8 min under these conditions. Electron backscattered imaging (BEI) was undertaken at 15 kV, 20 nA, and 1mm.

The five WD spectrometers of the probe permit almost complete in an age run monazite analysis. Spectral lines and elements were selected as follows: $K\alpha$ (Si, Al, Fe, Ca, and P), $L\alpha$ (La, Ce, Er, Yb, and Y), $L\beta$ (Pr, Nd, Sm, Gd, Tb, and Dy), $M\alpha$ (Th and Pb), and $M\beta$ (U). Total counting times, equally distributed for peak and background measurements, were 400 s (U, Pb), 200 s (Th), 60 s (Tb, Yb, and Er), 40 s (Si, Y, Sm, and Dy), and 20 s for the other elements.

Spectral line overlaps were carefully examined after wavelength scans over monazite samples and standards with special attention to age-determining elements. Fine tuning of background off-sets and pulse height settings allowed to avoid or minimize critical influences of the Th $M\zeta1$, Th $M\zeta2$, La $L\alpha$(II), other REE L lines, and S $K\alpha$ on Pb $M\alpha$, and the Th $M\gamma$ and other REE L lines on U $M\beta$. Our samples did not present detectable K and its effect on U $M\beta$ was disregarded. The Y $L\gamma$(2-3) overprint on Pb $M\alpha$ was corrected by an enhanced on-line procedure. Y contents in monazite are very low in garnet- or xenotime-bearing paragenesis and its influence is not a problem; in other cases, however, Y contents up to 2 wt. % may be found, sometimes also showing a remarkable Y zoning pattern.

Primary and secondary standards included synthetic ThO_2 (Th), UO_2 (U), PbO and the 95IRW Corning glass (Pb), $ThSiO_4$ (Si), YAl garnet (Y, Al), Ca_2P (Ca, P), REE phosphates and glasses (REE) and natural galena (Pb) and hematite (Fe). The NIST 610 and 612 reference glasses and a 610 *Ma.* old monazite (isotopic U-Pb age) were used for testing U, Th, and Pb settings. All measurements and age results herein refer to a 95% confidence level. X-ray counting uncertainties at 0.1, 0.1, and 4.0 wt. % Pb, U and Th contents were about 80, 110, and 320 ppm. Detection limits down to 60, 100, and 150 ppm, respectively, were attained in our analyses. Matrix effects were corrected with the PROZA procedure, as incorporated in the NORAN software.

AGE RESULTS AND DISCUSSION Up to 20 or 30 complete monazite point analysis were made for each sample taking single traverses on selected grains and individual spots in areas with high BEI contrast. Representative chemical and age data appear in Table 1. All analyses refer to monazite-Ce with variable within-grain and inter-grain Th, U, REE and Y contents. Within-grain zoning patterns revealed by BEI images are either normal (rare), oscillatory regular or irregular (in granites), or complex (some granites and metasedimentary rocks). Chemical variations are strongest in the MO-1216 granite, while the monazite from the Varginha granulite is very homogeneous. Age results are presented in graphical form in Figures 2 and 3 for granites and metamorphic rocks, respectively, by means mostly of their age distribution plots, but examples for 3D and 2D isochrons are also shown.

Monazite crystallization ages of the studied granites from the Alto Rio Grande Belt and the Socorro and Guaxupé Nappes are within a 600-625 Ma range. Samples from the Areia Branca Pluton (Morungaba) give independent Th-Pb and U-Pb chemical isochrons with ages of 619 ± 24 Ma and 623 ± 51 Ma, respectively (MO-1216), and a statistical average of 616 ± 14 Ma (MO-956). These results testify the reproducibility of the method, as the above samples came from the same petrographic unit. The accuracy of the results is also very good, as the chemical ages of this pluton fall within the expected 610-630 Ma range, well constrained by both stratigraphic and isochronic Rb/Sr data of related granite plutons (Vlach 1993). A similar age was obtained for the Nazaré Paulista granite (614 ± 14 Ma.), while the Pinhal granite from the Guaxupé domain appears to be somewhat younger (604 ± 10 Ma.); both results agree with recent monazite and zircon U-Pb isotopic data (Janasi 1999). The gneisses from Socorro and Varginha areas provide a remarkable evidence for more than one age population (Figure 3). A prominent statistical maximum at 625-630 (±20) Ma. for the Atibaia and Varginha samples clearly reflects the time of monazite crystallization and of the main metamorphism, as supported by rock textures. The equivalent maximum for the São Francisco Xavier (SFX) sample is younger, about 615 Ma, but still within error. In this sample monazite occurs mainly included in biotite and feldspars and such a result can be related to a possible late thermal resetting episode. Some monazite cores and small inclusions in garnet in all these metapelites gave results of 660-690 Ma, pointing to a possible inherited isotopic and chemical component or an incomplete homogenization due to a fast

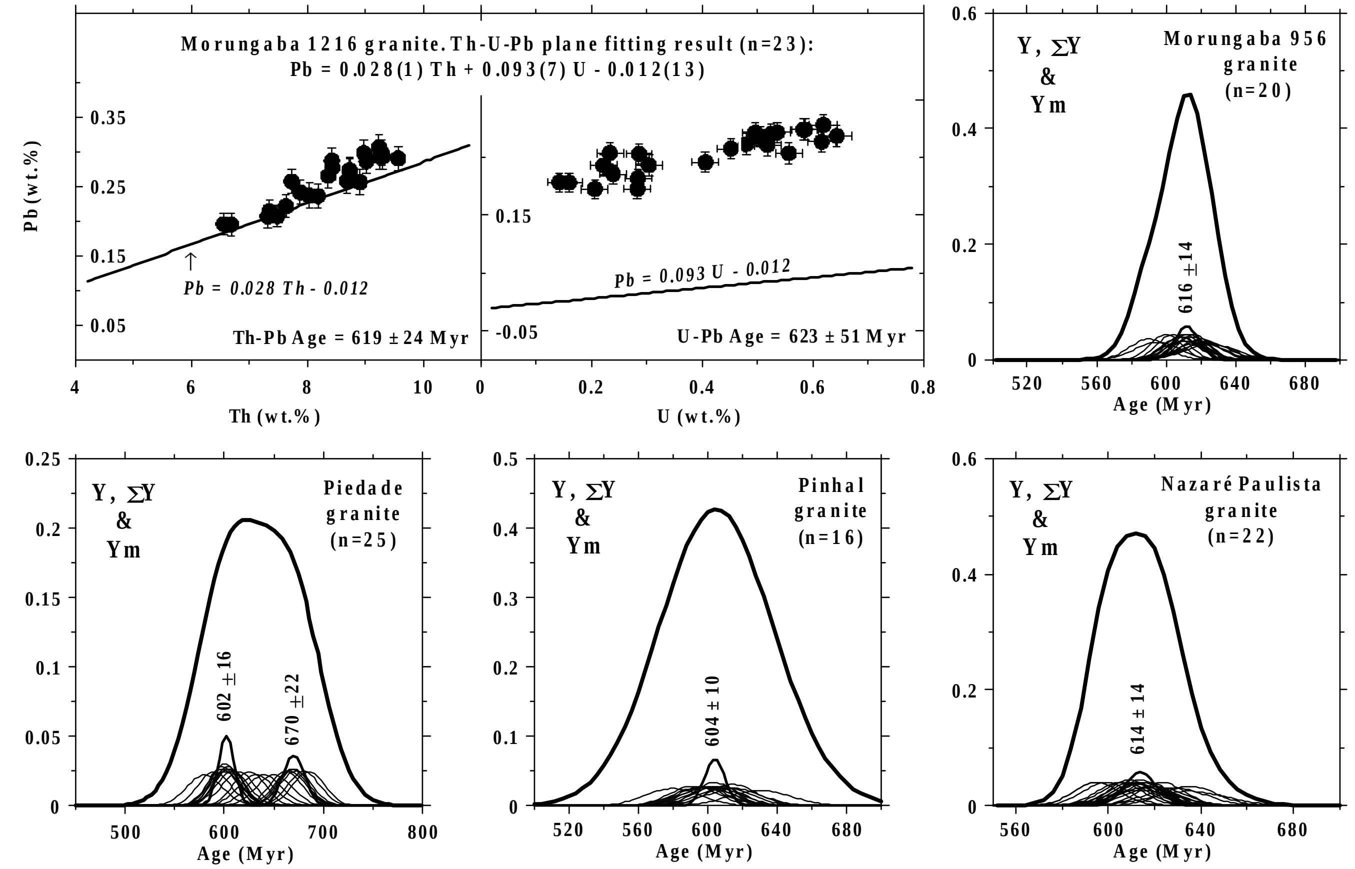

Figure 2 - Chemical isochronic and age distribution diagrams for studied granites from SE Brazil. Isochrons show direct projections of data points and the intersections of the 3D fit on Th-Pb and U-Pb sections. Y is the Gaussian probability density function of each spot, represented by thin lines; ΣY is the sum of all the Y functions, the "weighted hystogram" of a sample (coarse line), and Ym is the Y function for a significant population average.

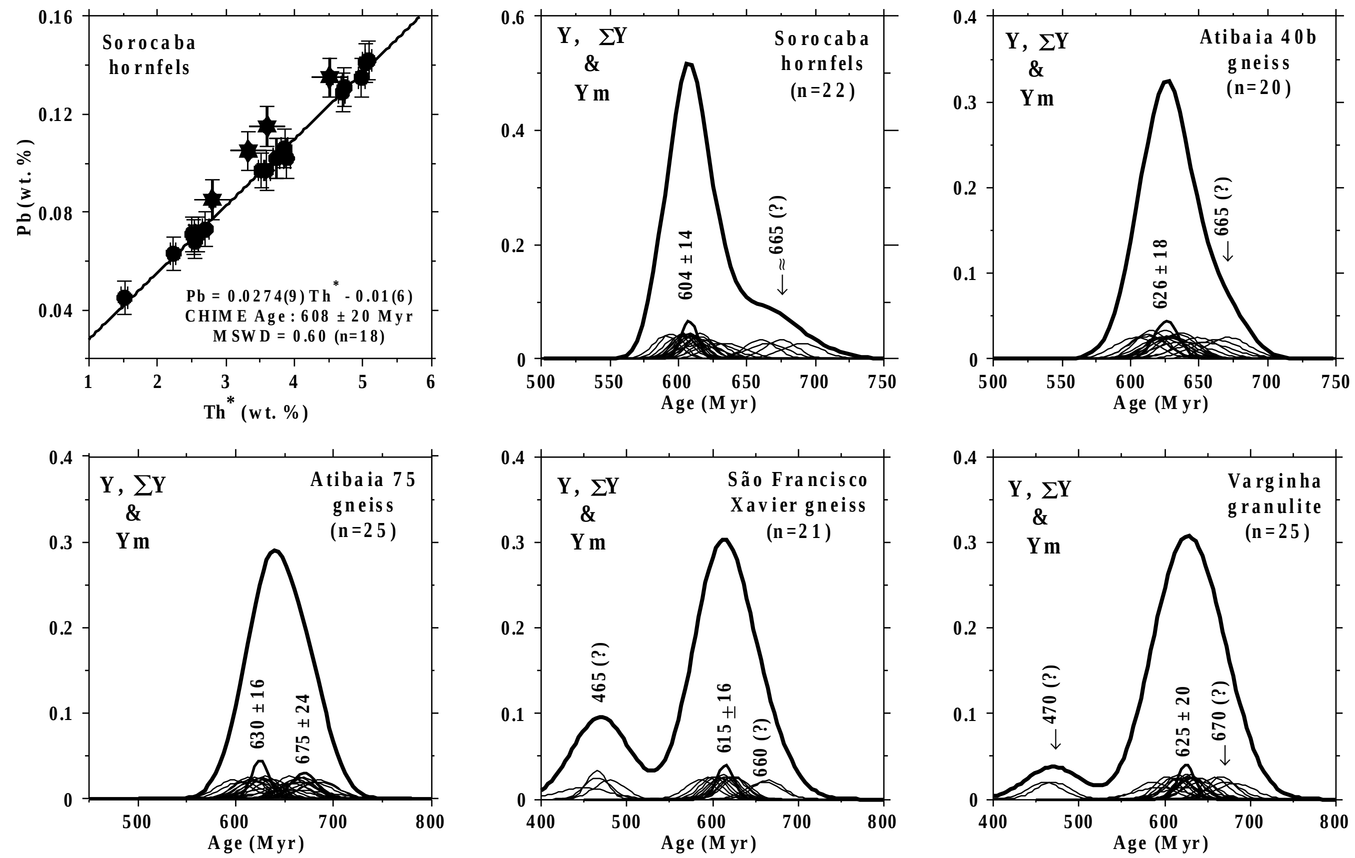

Figure 3 - 2D chemical isochronic and age distribution diagrams for the studied contact aureole and regional metamorphic rocks from SE Brazil. Th is the measured Th content plus the Th equivalent of the measured U for the iteratively computed isochronic age. Points represented by stars were not considered for line fitting. See Figure 1 for explanations on age distribution diagrams.*

Table 1 - Representative WDS monazite spot analysis and dating results for crust-derived granites and metamorphic rocks from SE Brazil.*

Sample	Morungaba MO-956		Morungaba MO-1216		Piedade PD-17		Pinhal, Nazaré Paulista		Sorocaba SO-02b		Atibaia A-40b		Atibaia A-75		São Francisco Xavier A-108		Varginha A-72O/b	
Wt.%	*C1n*	*C2n*	*C2n*	*C2b*	*C2-2*	*C2-5*	*PH,C1*	*NP,C1i*	*C1n*	*C2i*	*C1n*	*C1i*	*C1n*	*C1b*	*C1n*	*C1b*	*C1n*	*C1b*
SiO_2	0.89	1.08	1.04	0.65	0.07	0.33	0.40	0.80	0.38	0.31	0.18	0.07	0.31	0.19	0.34	0.21	0.22	0.26
ThO_2	5.57	6.85	9.58	5.88	4.54	3.53	7.97	5.84	5.16	2.29	5.73	3.12	5.04	4.13	8.29	6.42	4.56	4.79
UO_2	0.359	0.357	0.663	0.493	0.468	0.058	0.206	0.126	0.154	0.054	0.531	0.361	0.833	0.624	0.142	0.116	0.186	0.163
Al_2O_3	0.02	0.02	*bd*	0.02	*bd*	*bd*	*na*	*na*	0.02	0.02	0.02	0.05	0.02	0.03	0.07	0.08	*bd*	0.03
La_2O_3	17.76	16.28	14.58	16.59	16.57	16.91	14.75	17.48	12.31	16.54	13.84	13.73	15.08	14.60	12.91	12.51	13.76	15.21
Ce_2O_3	30.76	29.41	26.85	30.13	30.57	32.23	30.33	30.38	27.18	32.04	27.97	28.99	29.64	30.20	27.54	28.74	30.12	31.26
Pr_2O_3	2.83	2.73	2.57	2.87	2.93	3.06	3.15	2.95	3.10	3.20	3.03	3.13	3.39	3.40	3.20	3.37	3.38	3.25
Nd_2O_3	8.86	8.82	8.46	8.82	10.20	10.78	10.37	9.54	11.76	11.36	10.98	11.26	11.95	12.44	12.28	13.27	12.72	11.83
Sm_2O_3	1.26	1.45	1.35	1.21	1.48	1.52	1.48	1.23	2.22	1.37	1.97	2.03	1.83	1.87	2.10	2.40	2.06	1.56
Gd_2O_3	0.88	1.13	1.07	0.72	0.97	1.02	*na*	*na*	1.96	0.85	1.66	1.43	0.89	1.03	1.17	1.16	1.28	0.67
Tb_2O	*bd*	*bd*	*bd*	*bd*	*bd*	*bd*	*na*	*na*	0.14	0.08	0.17	0.19	*bd*	*bd*	0.11	0.05	*bd*	*bd*
Dy_2O	0.45	0.54	0.73	0.29	0.44	0.24	*na*	*na*	1.08	0.32	0.63	0.84	0.18	0.14	0.24	0.26	0.24	0.08
Er_2O_3	0.06	0.11	0.13	0.09	*bd*	*bd*	*na*	*na*	0.28	*bd*	*bd*	0.27	*bd*	*bd*	*bd*	*bd*	*bd*	*bd*
Yb_2O_3	0.10	*bd*	0.17	0.12	*bd*	0.09	*na*	*na*	0.19	0.10	0.08	0.23	0.09	0.09	0.09	0.09	0.08	*bd*
Y_2O_3	1.19	1.71	2.35	0.92	0.57	0.38	0.67	0.35	3.35	0.63	1.34	2.79	0.33	0.32	0.46	0.50	0.44	0.08
FeO	0.03	0.19	*bd*	*bd*	0.03	*bd*	*na*	*na*	*bd*	*bd*	0.05	*bd*	*bd*	*bd*	*bd*	0.02	*bd*	*bd*
CaO	0.39	0.55	1.13	0.89	1.01	0.16	0.50	0.75	0.76	0.30	1.21	0.71	0.99	0.85	1.47	1.18	0.81	0.84
PbO	0.173	0.212	0.316	0.192	0.157	0.100	0.222	0.163	0.162	0.064	0.219	0.113	0.206	0.169	0.220	0.175	0.140	0.139
P_2O_5	28.93	28.72	28.85	29.72	30.40	29.33	29.23	29.88	29.73	29.90	29.95	30.50	29.91	30.01	29.50	30.01	29.91	29.99
Sum	100.50	100.21	99.84	99.72	100.50	99.75	99.23	99.49	99.91	99.45	99.56	99.83	100.68	100.13	100.12	100.57	99.92	100.22
Spot Age	600 ± 30	620 ± 28	628 ± 26	604 ± 25	605 ± 30	630 ± 44	602 ± 27	610 ± 33	668 ± 34	603 ± 56	683 ± 30	615 ± 44	619 ± 27	640 ± 32	589 ± 28	602 ± 30	635 ± 37	611 ± 38
Spot Range	585 - 620		583 - 632		570 - 690		575-625	585-635	580 - 690		585 - 665		590 - 685		460 - 660		460 - 690	
Sample Age	616 ± 14		619 ± 24		602 ± 16		604 ± 10	614 ± 14	606 ± 16		626 ± 18		630 ± 16		615 ± 16		625 ± 20	

(*) Ages are given in Myr (95% confidence errors). Spot age: individual spot monazite crystallization age; Spot range: spot age range; Sample age: isochronic or statistical averaged sample age (see Figures 2 and 3). *Cn* = spot location; *bd* = below detection limit; *na* = not analysed.

crystal nucleation as monazite crystallization begun. Some thin rims in monazite grains included in feldspars from the SFX and Varginha gneisses gave very young and spurious dating results, close to 465 Ma, which must be related to some kind of Pb loss, perhaps induced by late fluid circulation.

To the southwest, in the Ribeira Belt domain, the Piedade granite sample shows also a marked bi-modal age distribution with maxima at 670 ± 22 Ma. and 602 ± 16 Ma. The former is clearly related to inheritance, as it appears in minor inclusions and clouded nuclei, while the latter, measured on their rims and other clean grains, undoubtedly reflects the main period of magma crystallization. The age for the Sorocaba Massif contact aureole, and so for the granite emplacement itself, is 604-608 ± 16 Ma. Again, the age diagram depicts some older results, at 660-670 Ma, a possible inheritance from the low-grade metamorphism of the São Roque Group.

GEOLOGICAL IMPLICATIONS AND FINAL COMMENTS

The EPMA age results suggest that the main medium- to high-grade metamorphic episode of the Socorro and Varginha nappe terranes occurred at about 620-630 Ma. Anatectic granite magmas in the Socorro and Guaxupé Nappes and the Alto Rio Grande Belt crystallized at 600-625 Ma. These results are in general agreement with recent isotopic data pointing to a similar age (622-626 Ma.) for both metamorphism and the related crustal-derived peraluminous magmatism (Janasi 1999, Campos Neto and Caby 1999). The former author interpreted some young isotopic monazite ages of similar granite samples (600-615 Ma.) as thermal overprints associated with the late evolved calcalkaline and A-type magmatism of the Itu Granite Province, at 610-590 Ma. (Vlach *et al.* 1990). Our data support such an interpretation and, in fact, a closer inspection of the MO-956 and the Nazaré Paulista age plots show indeed some asymmetry, with 590 and 620-630 Ma. age results, respectively. In any case, we suggest caution in assuming an isochronic character of all crustal granites in such terranes. The Piedade and the rapakivi-like Sorocaba granites from the Ribeira Belt gave similar younger ages (600-605 Ma.), which suggests that the main magmatism in this belt was younger, roughly synchronous with the late magmatism of the Itu Province in the nappe terranes. All studied metasedimentary rocks and the Piedade granite have possible inherit components of 690 Ma. that remain to be explained. It is worth emphasizing that similar results also appear in some monazite and zircon isotopic data (Janasi 1999).

Our results show that monazite chemical dating with the EPMA can give useful insights, highlighting the overall age picture within crustal belts in a fast and simple way, providing a very appropriate basis for further isotopic refinement. The relatively high errors (4% to 8% relative on individual spots, less on averages) are in great part superseded by the probe resolution, which allows to recognize contrasting age patterns even in intra-grain domains. The dating of metasedimentary rocks, migmatites and related granites is not a trivial job, as isotopic inheritance and incomplete homogenization are common features in rocks and their minerals. In such cases, micro-beam chemical (EPMA) and the more sophisticated isotopic (SHRIMP) dating methods will play a very significant role to understand details of the geologic history.

Acknowledgments To Fundação de Amparo à Pesquisa do Estado de São Paulo and Conselho Nacional de Pesquisa for support. F.A. Negri and M.C. Campos Neto provided some of the samples. H. Ulbrich, I. McReath, and two anonymous referees of Revista Brasileira de Geociências kindly reviewed the manuscript.

References

Crowley J.L. and Ghent E.D. 1999. An electron microprobe study of the U-Th-Pb systematics of metamorphosed monazite: the role of Pb diffusion versus overgrowth and recrystallization. *Chemical Geology*, **157**:285-302.

Campos Neto M.C. and Caby R. 1999. Neoproterozoic high-pressure metamorphism and tectonic constraint from the nappe system south of the São Francisco Craton, southeast Brazil. *Precambrian Research*, **97**:3-26.

Janasi V.A. 1999. Petrogênese de granitos crustais na Nappe de empurrão Socorro-Guaxupé (SP-MG): uma contribuição da geoquímica elemental e isotópica. Unpublished Livre-Docência thesis. Inst. de Geociências, Universidade de São Paulo, São Paulo. 304 p.

Montel J.-M., Foret S., Veschambre M., Nicollet C., Provost A. 1996. Electron microprobe dating of monazite. *Chemical Geology*, **131**:37-53.

Parrish R.R. 1990. U-Pb dating of monazite and its applications to geological problems. *Canadian Journal of Earth Sciences*, **32**:1618-1642.

Podor R. and Cuney M. 1997. Experimental study of Th-bearing $LaPO_4$ (780° C, 200 MPa): implications for monazite and actinide orthophosphate stability. *American Mineralogist*, **82**:765-771.

Rhede D., Wendt I., Forster H.J. 1996. A three-dimensional method for calculating independent chemical U/Pb and Th/Pb-ages of accessory minerals. *Chemical Geology*, **130**:247-253.

Susuki K. and Adachi M. 1991. Precambrian provenance and Silurian metamorphism of the Tsunosawa paragneiss in the South Kitakami terrane, Northeast Japan, revealed by the chemical Th-U-total Pb isochron ages of monazite, zircon, and xenotime. *Geochemical Journal*, **25**:277-292.

Vlach S.R.F. 1993. Geologia e Petrologia dos granitóides da região de Morungaba, São Paulo. Unpublished doctoral thesis. Inst. de Geociências, Universidade de São Paulo, São Paulo. 414 p.

Vlach S.R.F., Gualda G.A.R., Chiessi C.M. 1999. Electron microprobe monazite dating: first results for two granites from Southeastern Brazil. *In*: South American Symposium on Isotope Geology, 2. *Actas*...Cordoba, Argentina, 518-521.

Vlach S.R.F., Janasi V.A., Vasconcellos A.C.B.C. 1990. The Itu Belt: associated calc-alkaline and aluminous A-type late Brasiliano granitoids in the states of São Paulo and Paraná, southern Brazil. *In*: Congresso Brasileiro de Geologia, 36. *Anais*...Natal, SBG, **4**:1700-1711.

Contribution IGC-098
Received March 1, 2000
Accepted for publication April 5, 2000